

# The Wolff Rearrangement: The Relevant Portion of the Oxirene–Ketene Potential Energy Hypersurface

Anthony P. Scott,<sup>1a</sup> Ross H. Nobes,<sup>1b</sup> Henry F. Schaefer III,<sup>\*,1c</sup> and Leo Radom<sup>\*,1a</sup>

Contribution from the Research School of Chemistry, Australian National University, Canberra, ACT 0200, Australia, Australian National University Supercomputer Facility, Canberra, ACT 0200, Australia, and Center for Computational Quantum Chemistry, University of Georgia, Athens, Georgia 30602

Received May 10, 1994<sup>⊙</sup>

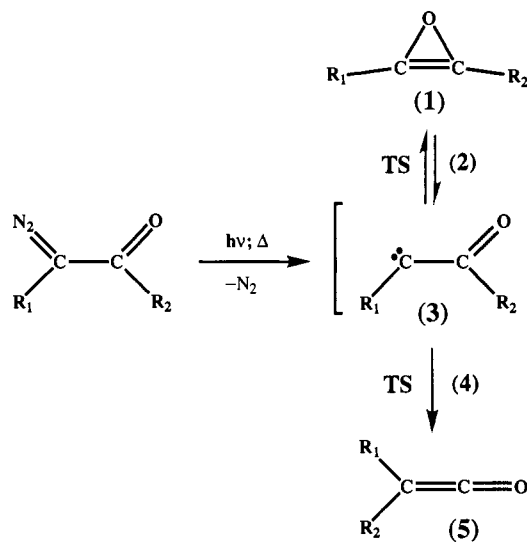
**Abstract:** The portion of the C<sub>2</sub>H<sub>2</sub>O potential energy hypersurface that includes oxirene, formylmethylene, and ketene has been studied with *ab initio* methods incorporating high levels of electron correlation and basis sets that include up to f and g functions. Our best geometries were determined at the CCSD(T)/6-311G(df,p) level of theory. Single-point energies were then determined by using CCSD(T) and BD(T) calculations with the cc-pVTZ basis set augmented with additional f and g polarization functions. Our main conclusion is that there is little or no barrier separating formylmethylene from oxirene, the potential energy surface linking these two species being extremely flat. On the other hand, a more significant barrier (21–23 kJ mol<sup>-1</sup>) separates formylmethylene or oxirene from ketene. These results strongly support the previously postulated intermediacy of oxirene in the Wolff rearrangement. Ketene is found to lie 325 kJ mol<sup>-1</sup> lower in energy than oxirene. Our predicted energy threshold for the scrambling of carbon atoms in ketene (348 kJ mol<sup>-1</sup>) is in close agreement with a recent experimental value (340 kJ mol<sup>-1</sup>).

## Introduction

Despite its synthetic utility and long history, the Wolff rearrangement<sup>2</sup> (typified by Scheme 1) is still not fully understood.

The Wolff rearrangement has been the focus of a review<sup>3</sup> and numerous experimental<sup>4–9</sup> and theoretical<sup>10–16</sup> studies. The mechanism is generally thought to involve the formation of a ketocarbene intermediate (3) by the photolysis (or thermolysis) of diazoketones. The ketocarbene undergoes rearrangement to a ketene (5). The participation of symmetrical intermediates,

## Scheme 1



\* Abstract published in *Advance ACS Abstracts*, October 1, 1994.

(1) (a) Research School of Chemistry, Australian National University. (b) Australian National University Supercomputer Facility. (c) University of Georgia.

(2) Wolff, L. *Justus Liebigs Ann. Chem.* **1902**, 325, 129; **1912**, 394, 23.

(3) Meier, H.; Zeller, K.-P. *Angew. Chem., Int. Ed. Engl.* **1975**, 14, 32.

(4) (a) Csizmadia, I. G.; Font, J.; Strausz, O. P. *J. Am. Chem. Soc.* **1968**, 90, 7360. (b) Thornton, D. E.; Gosavi, R. K.; Strausz, O. P. *J. Am. Chem. Soc.* **1970**, 92, 1768. (c) Zeller, K.-P. *Angew. Chem., Int. Ed. Engl.* **1977**, 11, 781.

(5) (a) Russell, R. L.; Rowland, F. S. *J. Am. Chem. Soc.* **1970**, 92, 7508. (b) Lovejoy, E. R.; Kim, S. K.; Alvarez, R. A.; Moore, C. B. *J. Chem. Phys.* **1991**, 95, 4081. (c) Lovejoy, E. R.; Moore, C. B. *J. Chem. Phys.* **1993**, 98, 7846.

(6) (a) Matlin, S. A.; Sammes, P. G. *J. Chem. Soc. Chem. Commun.* **1972**, 11. (b) Matlin, S. A.; Sammes, P. G. *J. Chem. Soc., Perkin Trans. 1* **1972**, 2623. (c) Matlin, S. A.; Sammes, P. G. *J. Chem. Soc., Perkin Trans. 1* **1973**, 2851.

(7) Tanigaki, K.; Ebbesen, T. W. *J. Am. Chem. Soc.* **1987**, 109, 5883.

(8) (a) Debu, F.; Monnier, M.; Verlaque, P.; Davidovics, G.; Pourcin, J.; Bodot, H.; Aycard, J.-P. *C. R. Acad. Sci. Paris, Ser. 2* **1986**, 303, 897. (b) Bachman, C.; N'Guessan, T. Y.; Debu, F.; Monnier, M.; Pourcin, J.; Aycard, J.-P.; Bodot, H. *J. Am. Chem. Soc.* **1990**, 112, 7488.

(9) See, for example: (a) Hayes, R. A.; Hess, T. C.; McMahon, R. J.; Chapman, O. L. *J. Am. Chem. Soc.* **1983**, 105, 7786. (b) McMahon, R. J.; Chapman, O. L.; Hayes, R. A.; Hess, T. C.; Krimmer, H. P. *J. Am. Chem. Soc.* **1985**, 107, 7597.

(10) Csizmadia, I. G.; Gunning, H. E.; Gosavi, R. K.; Strausz, O. P. *J. Am. Chem. Soc.* **1973**, 95, 133.

(11) Dewar, M. J. S.; Ramsden, C. A. *J. Chem. Soc., Chem. Commun.* **1973**, 688.

(12) (a) Strausz, O. P.; Gosavi, R. K.; Gunning, H. E. *J. Chem. Phys.* **1977**, 67, 3057. (b) Strausz, O. P.; Gosavi, R. K.; Gunning, H. E. *Chem. Phys. Lett.* **1978**, 54, 510.

(13) Dykstra, C. E. *J. Chem. Phys.* **1978**, 68, 4244.

(14) Strausz, O. P.; Gosavi, R. K.; Denes, A. S.; Csizmadia, I. G. *J. Am. Chem. Soc.* **1976**, 98, 4784.

(15) Tanaka, K.; Yoshimine, M. *J. Am. Chem. Soc.* **1980**, 102, 7655.

(16) Bouma, W. J.; Nobes, R. H.; Radom, L.; Woodward, C. E. *J. Org. Chem.* **1982**, 47, 1869.

such as oxirenes (1), has been proposed on the basis of <sup>13</sup>C labeling experiments where diazoketones, labeled at the carbonyl carbon, were found to give rise to ketenes (5) that bore the label at both carbon atoms.<sup>4</sup> Other researchers have investigated the role played by oxirene-like structures during the retro-Wolff rearrangement.<sup>5</sup> Lovejoy *et al.*<sup>5b,c</sup> in particular have recently studied the role of a symmetrical oxirene species in the isomerization of vibrationally excited ketene.

In the thermolysis of diazoketones, the participation of oxirenes appears to be small at low temperatures where ketocarbenes play a greater role. The symmetrical oxirene species, however, become more important as the temperature increases.<sup>5</sup> This has been interpreted as indicating that ketocarbene-like structures are energetically more stable than oxirenes.

The "stable" structures that have often been proposed to be involved in the rearrangement have been studied in detail individually. The parent ketene (or ethenone) (5, R<sub>1</sub> = R<sub>2</sub> = H) is a well-characterized molecule. Its structure and vibrational frequencies have been determined experimentally<sup>17–20</sup> and theoretically.<sup>21</sup> Formylmethylene (3, R<sub>1</sub> = R<sub>2</sub> = H) has yet to be

observed experimentally although it has been studied by theoretical means.<sup>22</sup> There have been numerous experimental studies, however, of various substituted ketocarbenes.<sup>8,9</sup> Unsubstituted oxirene likewise has yet to be observed experimentally, but Bodot *et al.*<sup>8</sup> have inferred the existence of dimethyloxirene (**1**,  $R_1 = R_2 = \text{CH}_3$ ) during the photolysis of 3-diazo-2-butanone. The most complete theoretical discussion of the parent oxirene (**1**,  $R_1 = R_2 = \text{H}$ ) is that of Vacek *et al.*<sup>23,24</sup>

The most comprehensive previous theoretical studies of the mechanism of the Wolff rearrangement have been those by Tanaka and Yoshimine<sup>15</sup> and by Bouma *et al.*<sup>16</sup> These studies showed that at the Hartree–Fock level **3** was more stable than **1** by 50–71 kJ mol<sup>-1</sup>. However, when electron correlation was included through single-point calculations at the Hartree–Fock optimized structures, the energy difference was reduced substantially to 4–33 kJ mol<sup>-1</sup>. The barrier to ring opening for oxirene has been predicted to be less than 31 kJ mol<sup>-1</sup> by a number of *ab initio* studies.<sup>12–16</sup> The best estimate to date is possibly that of Tanaka and Yoshimine,<sup>15</sup> who, through a reaction coordinate approach, predicted a barrier of 8 kJ mol<sup>-1</sup>. The ring deformation vibrational frequency for **1** has been shown to be strongly dependent on the level of electron correlation and the size of the basis set.<sup>24</sup> The best current prediction is that of Vacek *et al.*,<sup>24</sup> who obtained a  $b_2$  vibrational frequency of 139 cm<sup>-1</sup> at the CCSD(T)/cc-pVTZ level of theory. Such a soft vibration suggests a low barrier for the rearrangement of **1** to **3**.

The rearrangement of formylmethylene (**3**) to ketene (**5**) via **4** has also received theoretical attention.<sup>15,16</sup> At the Hartree–Fock level, a barrier of 16 kJ mol<sup>-1</sup> has been found for the rearrangement of **3** to **5**. However, on inclusion of electron correlation (MP2 and MP3), the rearrangement transition structure (**4**) was predicted to lie lower in energy than **3**. Such a finding suggests that the rearrangement of **3** to **5** may occur without an energy barrier and that entry into the Wolff rearrangement at **3** would result in spontaneous isomerization to **5**.

Most of the previous theoretical work dealing with the Wolff rearrangement surface has used relative energies calculated at correlated levels with geometries determined at the Hartree–Fock level. The validity of such an approach relies on the assumption that little change in the geometry of the stationary points will occur with increasing sophistication of the theoretical procedure. It is clearly preferable to use geometries obtained with correlated methods, particularly in cases (such as the Wolff rearrangement) where the potential energy surface is seen to be sensitive to the level of theory employed. To overcome the limitations of previous work on the Wolff rearrangement, there is a pressing need for a high-level theoretical exploration of the oxirene → ketene potential energy surface. In the present paper, we describe the results of such an investigation.

## Theoretical Methods

The stationary points **1**–**5** ( $R_1 = R_2 = \text{H}$ ) indicated in Scheme 1 were fully optimized using analytic gradient techniques for restricted Hartree–Fock (RHF), density functional theory (DFT) (using the gradient-

corrected B-LYP<sup>25</sup> and the hybrid Becke3-LYP<sup>26,27</sup> functionals), second-order Møller–Plesset perturbation theory (MP2), and coupled-cluster (CCSD(T)) wave functions. Geometry optimizations for the RHF, MP2, and DFT methods were carried out with the Gaussian 92/DFT program.<sup>27,28</sup> All the CCSD(T) geometry optimizations were carried out with the ACES II program.<sup>29</sup> Calculations for post-Hartree–Fock methods were performed with all orbitals correlated. The nature of the stationary points found with the RHF, DFT, MP2, and some of the CCSD(T) procedures was determined by calculation of harmonic vibrational frequencies. Analytical methods for the calculation of the second derivatives were employed for the RHF,<sup>30</sup> MP2,<sup>31</sup> and DFT<sup>32</sup> methods. The second derivatives for the CCSD(T) procedure were calculated by finite central differences of the gradients.

Our best geometries were obtained at the CCSD(T)/6-311G(df,p) level of theory. It should be noted that, whereas the 6-31G(d), 6-31G(d,p), and 6-311G(d,p) basis sets were used in their standard form<sup>33</sup> in the present work, our 6-311G(df,p) basis<sup>34,35</sup> is nonstandard in that we use all six second-order and all ten third-order Cartesian functions rather than the more usual pure angular momentum polarization functions.<sup>36</sup>

Determination of harmonic vibrational frequencies at the CCSD(T)/6-311G(df,p) level, although desirable, would have been prohibitively time consuming for the  $C_1$  stationary points in the absence of analytical second derivatives, using our current resources. Instead, we have calculated harmonic vibrational frequencies at the CCSD(T)/6-31G(d) level. As will be seen in later sections of this paper, the energy hypersurface at this level of theory has the same qualitative shape around the  $C_2$  oxirene structure as that calculated at CCSD(T)/6-311G(df,p), lending support to this approach. In addition, the geometries for the individual stationary points at the CCSD(T)/6-31G(d) level are generally quite similar to those calculated at CCSD(T)/6-311G(df,p). Previous reports<sup>37</sup> have shown that harmonic vibrational frequencies calculated with the CCSD(T) procedure and with reasonable sized basis sets give very good agreement with observed (anharmonic) vibrational frequencies.

The connections between the stationary points **1**–**5** on the potential surface were confirmed through linear synchronous transit (LST) calculations at the CCSD(T)/6-31G\* level. The LST calculations showed monotonic energy changes between structures **1** and **2**, **2** and **3**, **3** and **4**, and **4** and **5**.

Additional single-point energy calculations using larger basis sets were performed at the CCSD(T)/6-311G(df,p) optimized geometries with

(25) (a) Johnson, B. G.; Gill, P. M. W.; Pople, J. A. *J. Chem. Phys.* **1992**, *97*, 7846. (b) Johnson, B. G.; Gill, P. M. W.; Pople, J. A. *J. Chem. Phys.* **1993**, *98*, 5612. (c) Gill, P. M. W.; Johnson, B. G.; Pople, J. A.; Frisch, M. J. *Chem. Phys. Lett.* **1992**, *197*, 499.

(26) This involves Becke's three-parameter functional with the non-local correlation provided by the LYP expression which results in the correlation functional being expressed as  $C_E^{\text{LYP}} + (1 - C) E_c^{\text{VWN}}$ .

(27) Gaussian 92/DFT, Revision F.3. Frisch, M. J.; Trucks, G. W.; Schlegel, H. B.; Gill, P. M. W.; Johnson, B. G.; Wong, M. W.; Foresman, J. B.; Robb, M. A.; Head-Gordon, M.; Replogle, E. S.; Gomperts, R.; Andres, J. L.; Raghavachari, K.; Binkley, J. S.; Gonzalez, C.; Martin, R. L.; Fox, D. J.; DeFrees, D. J.; Baker, J.; Stewart, J. J. P.; Pople, J. A. Gaussian Inc.: Pittsburgh, PA, 1993.

(28) The default SG-1 grid was used: Gill, P. M. W.; Johnson, B. G.; Pople, J. A. *Chem. Phys. Lett.* **1993**, *209*, 506.

(29) (a) ACES II, Version 0.2. Stanton, J. F.; Gauss, J.; Watts, J. D.; Lauderdale, W. J.; Bartlett, R. J. Quantum Theory Project: University of Florida, 1992. (b) Stanton, J. F.; Gauss, J.; Watts, J. D.; Lauderdale, W. J.; Bartlett, R. J. *Int. J. Quantum. Chem. Symp.* **1992**, *26*, 879.

(30) Saxe, P.; Fox, D. J.; Schaefer, H. F.; Handy, N. C. *J. Chem. Phys.* **1982**, *77*, 5584.

(31) Schlegel, H. B.; Binkley, J. S.; Pople, J. A. *J. Chem. Phys.* **1984**, *80*, 1976.

(32) (a) Johnson, B. G.; Frisch, M. J. *Chem. Phys. Lett.* **1993**, *216*, 133. (b) See also: Handy, N. C.; Tozer, D. J.; Laming, G. J.; Murray, C. W.; Amos, R. D. *Isr. J. Chem.* **1993**, *33*, 331.

(33) (a) Hariharan, P. C.; Pople, J. A. *Theor. Chim. Acta* **1973**, *28*, 213. (b) Krishnan, R.; Binkley, J. S.; Seeger, R.; Pople, J. A. *J. Chem. Phys.* **1980**, *72*, 650.

(34) Frisch, M. J.; Pople, J. A.; Binkley, J. S. *J. Chem. Phys.* **1984**, *80*, 3265.

(35)  $\alpha(\text{C}) = 0.8$  and  $\alpha(\text{O}) = 1.4$ .

(36) We used this approach because of limitations in the analytical gradient procedures that are coded in the ACES II program.

(37) Average errors in calculated harmonic vibrational frequencies are as follows: CCSD(T)/DZP 1.5%, CCSD(T)/TZ2P 1.1%, CCSD(T)/TZ(2df-2p) 0.6%, CCSD(T)/cc-pVDZ 27 cm<sup>-1</sup>, CCSD(T)/cc-pVTZ 12 cm<sup>-1</sup>, and CCSD(T)/cc-pVQZ 9 cm<sup>-1</sup>. See: (a) Thomas, J. R.; DeLeeuw, B. J.; Vacek, G.; Schaefer, H. F. *J. Chem. Phys.* **1993**, *98*, 1336. (b) Thomas, J. R.; DeLeeuw, B. J.; Vacek, G.; Crawford, T. D.; Yamaguchi, Y.; Schaefer, H. F., III *J. Chem. Phys.* **1993**, *99*, 403. (c) Martin, J. M. L. *J. Chem. Phys.* In press. Preprint obtained from JCP express 001411.

(17) Duncan, J. L.; Ferguson, A. M.; Harper, J.; Tonge, K. H. *J. Mol. Spectrosc.* **1987**, *125*, 196.

(18) Brown, R. D.; Godfrey, P. D.; McNaughton, D.; Pierlot, A. P.; Taylor, W. H. *J. Mol. Spectrosc.* **1990**, *140*, 340.

(19) Moore, C. B.; Pimentel, G. C. *J. Chem. Phys.* **1963**, *38*, 2816.

(20) Mallinson, P. D.; Nemes, L. *J. Mol. Spectrosc.* **1976**, *59*, 470.

(21) See, for example: (a) Allen, W. D.; Schaefer, H. F. *J. Chem. Phys.* **1986**, *84*, 2212. (b) Leszczynski, J.; Kwiatkowski, J. S. *Chem. Phys. Lett.* **1993**, *201*, 79.

(22) See, for example: (a) Baird, N. C.; Taylor, K. F. *J. Am. Chem. Soc.* **1978**, *100*, 1333. (b) Nova, J. J.; McDouall, J. J. W.; Robb, M. A. *J. Chem. Soc., Faraday Trans. 2* **1987**, *83*, 1629. (c) Gosavi, R. K.; Torres, M.; Strausz, O. P. *Can. J. Chem.* **1991**, *69*, 1630.

(23) Vacek, G.; Colegrove, B. T.; Schaefer, H. F. *Chem. Phys. Lett.* **1991**, *177*, 468.

(24) Vacek, G.; Galbraith, J. M.; Yamaguchi, Y.; Schaefer, H. F.; Nobes, R. H.; Scott, A. P.; Radom, L. *J. Phys. Chem.* in press.

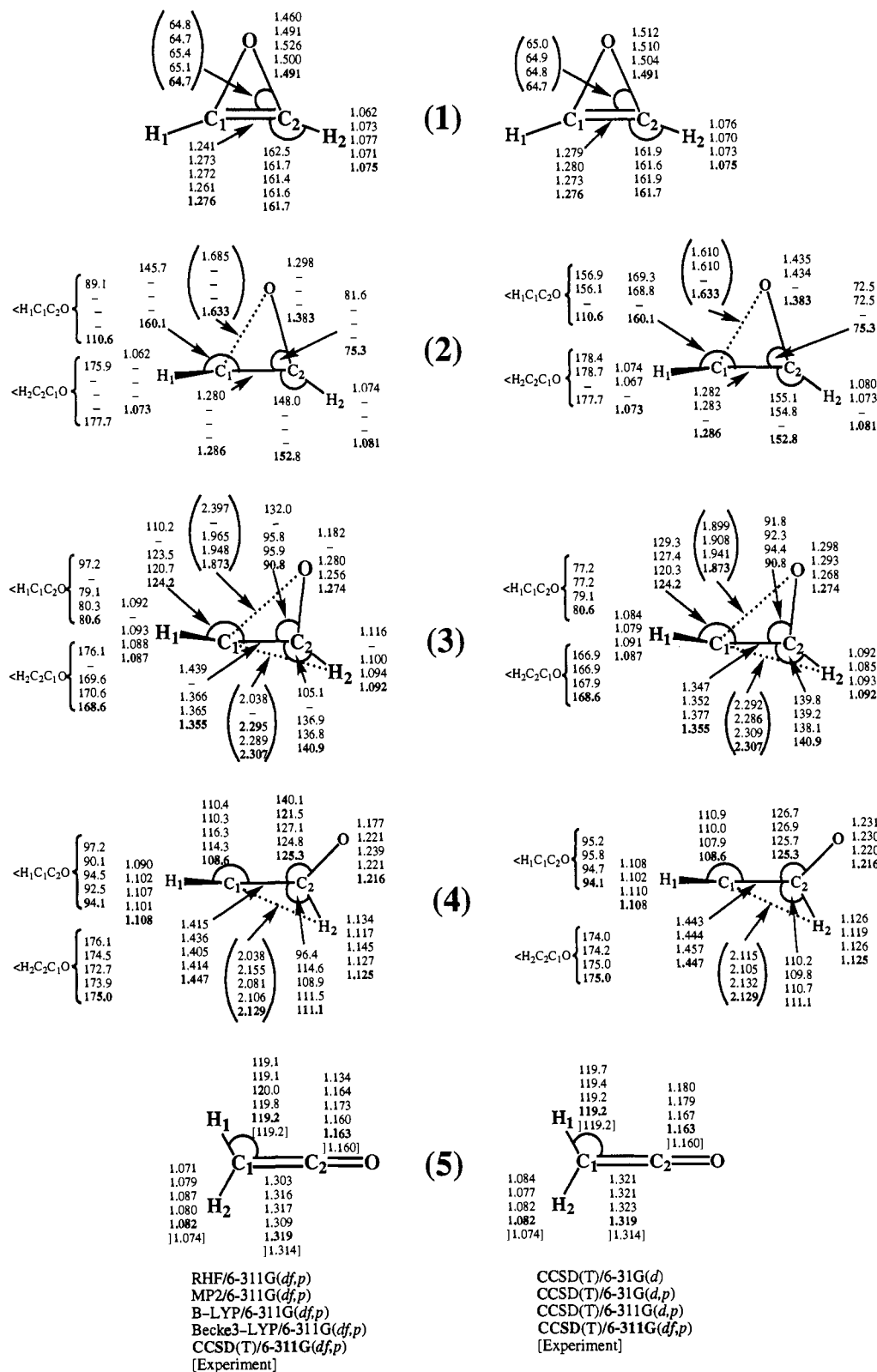


Figure 1. Optimized molecular structures for 1–5.

the MOLPRO program.<sup>38</sup> Such calculations were carried out by using the CCSD(T) method or the Brueckner doubles method with perturbative inclusion of triple excitations (BD(T)). We have employed the Dunning correlation-consistent basis, cc-pVTZ,<sup>39,40</sup> as our “standard” larger set. Two still larger basis sets have been built from the cc-pVTZ basis to

(38) MOLPRO is a package of *ab initio* programs written by H.-J. Werner, P. J. Knowles, with contributions of J. Almlof, R. D. Amos, S. T. Elbert, K. Hampel, W. Meyer, K. Peterson, R. M. Pitzer, and A. J. Stone. See also: Hampel, C.; Peterson, K.; Werner, H.-J. *Chem. Phys. Lett.* **1992**, *190*, 1.

(39) Dunning, T. H. *J. Chem. Phys.* **1989**, *90*, 1007.

(40) (10s5p2d1f)/[4s3p2d1f].

investigate the effect of further basis set enhancements. The pVTZ(f) basis was constructed by the addition<sup>34</sup> of another shell of *f* polarization functions to make a [4s3p2d2f] basis. The pVTZ(g) basis was constructed by the addition of a *g* shell to the standard cc-pVTZ basis resulting in a [4s3p2d1f1g] basis. The exponent for the *g* shell was obtained from the Dunning correlation-consistent cc-pVQZ basis<sup>39,41</sup> and used without further optimization.

All results reported in this paper correspond to calculations based on the restricted formulations of Hartree–Fock or density functional theory.

(41) (12s6p3d2f1g)/[5s4p3d2f1g].

**Table 1.** Harmonic Vibrational Frequencies and Infrared Intensities<sup>a</sup>

oxirene (1)			TS(1→3) (2)		formylmethylene (3)		TS(3→5) (4)		ketene (5)		
sym	freq	int	freq	freq	int	freq	sym	freq	int	expt <sup>b</sup>	
<i>b</i> <sub>2</sub>	21	0.5	133i	328	21.8	409i	<i>b</i> <sub>2</sub>	438	3.1	443	
<i>a</i> <sub>2</sub>	396	0.0	179	455	220.0	508	<i>b</i> <sub>1</sub>	508	70.9	539	
<i>b</i> <sub>1</sub>	451	79.0	632	677	74.9	727	<i>b</i> <sub>1</sub>	593	75.8	593	
<i>a</i> <sub>1</sub>	870	39.5	809	951	6.9	945	<i>b</i> <sub>2</sub>	1018	6.3	998	
<i>b</i> <sub>2</sub>	931	6.8	955	1178	28.8	1076	<i>a</i> <sub>1</sub>	1167	8.0	1133	
<i>a</i> <sub>1</sub>	1081	2.2	1146	1408	24.6	1387	<i>a</i> <sub>1</sub>	1445	13.1	1416	
<i>a</i> <sub>1</sub>	1781	1.0	1773	1565	14.0	1692	<i>a</i> <sub>1</sub>	2217	445.8	2185	
<i>b</i> <sub>2</sub>	3343	27.9	3322	3187	14.2	2795	<i>a</i> <sub>1</sub>	3218	20.9	3215	
<i>a</i> <sub>1</sub>	3410	1.5	3426	3285	8.0	3026	<i>b</i> <sub>2</sub>	3316	3.8	3308	

<sup>a</sup> Calculated at the CCSD(T)/6-31G(d) level. Harmonic vibrational frequencies in cm<sup>-1</sup>, infrared intensities in km mol<sup>-1</sup>. <sup>b</sup> Experimental frequencies from ref 17.

In fact, structures 1–4 all have lower-energy UHF (compared with RHF) solutions. However, at the CCSD(T) level, the RCCSD(T) energies for 1–4 are found to be uniformly lower than the UCCSD(T) energies.<sup>42</sup>

Throughout this paper, bond lengths are given in ångströms and bond angles in degrees. Non-independent geometrical parameters in Figure 1 are displayed in parentheses.

## Results and Discussion

**Structures and Frequencies.** The equilibrium geometries for 1–5, obtained at the RHF, MP2, B-LYP, Becke3-LYP, and CCSD(T) levels of theory with the 6-311G(df,p) basis, are displayed on the left-hand side of Figure 1. These results serve to illustrate the dependence of the geometries on the level of incorporation of electron correlation. In addition, we present on the right-hand side of Figure 1 the geometries for 1–5 with the CCSD(T) procedure and the 6-31G(d), 6-31G(d,p), 6-311(d,p), and 6-311G(df,p) basis sets. These results show the effect of increasing the size of the basis set on the geometrical structures.

**(A) Oxirene (1).** Oxirene has been studied extensively in two very recent papers.<sup>23,24</sup> In the more comprehensive study of the oxirene molecule,<sup>24</sup> geometries were obtained with the CCSD(T) procedure and basis sets up to cc-pVTZ. In the context of the present work, we note that increasing the level of theory from RHF to MP2 causes the most substantial change in the geometry for 1. Little change occurs on progressing further to CCSD(T). The DFT procedures predict a C–O bond rather longer than that of the other methods. The basis set effect is smaller but a gradual shortening of the C–O bond can be seen in going from 6-31G(d) to 6-311G(df,p). It is interesting that at the B-LYP, Becke3-LYP, and CCSD(T)/6-311G(d,p) levels of theory, 1 is a saddle point with one imaginary frequency corresponding to an in-plane, ring-opening motion of the heavy atom framework. At the other levels of theory, 1 is predicted to be a minimum on the potential energy surface. Our predicted harmonic vibrational frequencies at the CCSD(T)/6-31G(d) level of theory are presented in Table 1. It has previously been noted<sup>23,24</sup> that the ring-opening (*b*<sub>2</sub>) vibrational frequency for 1 is very sensitive to the level of theory employed. Indeed, while at the CCSD(T)/6-31G(d) level the in-plane ring deformation frequency is calculated to be 21 cm<sup>-1</sup>, at the CCSD(T)/6-311G(df,p) level this frequency is predicted<sup>24</sup> to be 137 cm<sup>-1</sup>.

**(B) Formylmethylene (3).** Formylmethylene has been studied in detail by a number of researchers<sup>22</sup> at varying levels of theory. Gosavi *et al.*<sup>22c</sup> have reported RHF/6-31G(d,p) and CISDQ/6-31G(d,p) optimized structures for the low-lying electronic states of 3. They find, in accord with the results of Bouma *et al.*,<sup>16</sup> that 3 is nonplanar and that it is a minimum on the Hartree–Fock surface. Our calculated vibrational frequencies (Table 1) show that 3 is also a genuine minimum on the CCSD(T)/6-31G(d) potential energy surface.

**(C) Ketene (5).** Ketene has been studied recently at the MP2/TZP level of theory by Leszczynski and Kwiatkowski.<sup>21b</sup> Their

geometry, rotational constants, and harmonic vibrational frequencies agree well with those determined by experiment. Inspection of Figure 1 reveals that the RHF/6-311G(df,p) C–O and C–C bond lengths for 5 are shorter than the experimental values. This deficiency is rectified by the inclusion of electron correlation at the MP2 level. The geometry predicted at the CCSD(T) level of theory differs only slightly from that predicted at the MP2 level. Of the two DFT methods, the Becke3-LYP method gives the better prediction of geometry. Our CCSD(T)/6-31G(d) harmonic vibrational frequencies for 5 (Table 1) are in excellent agreement with experiment.

**(D) TS(1→3) (2).** We were able to locate the transition structure (2) linking oxirene (1) and formylmethylene (3) at the HF/6-311G(df,p), CCSD(T)/6-31G(d), CCSD(T)/6-31G(d,p), and CCSD(T)/6-311G(df,p) levels of theory. At MP2/6-311G(df,p), even after an exhaustive search, we could not find a stationary point that corresponds to a structure like 2. On the other hand, both the DFT methods and CCSD(T)/6-311G(d,p) predict that 1 is a transition structure which precludes the existence of 2 at these levels of theory. All those methods that do predict the existence of 2 show it to be of C<sub>1</sub> symmetry. The partially-ring-opened C–O bond is predicted to be about 1.6 Å in length (*cf.* about 1.5 Å in 1). Structure 2 is predicted to be very nonplanar, with the ∠H<sub>1</sub>C<sub>1</sub>C<sub>2</sub>O dihedral angle being about 111° at our best level of theory. An interesting observation is, however, that the smaller 6-31G basis sets, with the CCSD(T) procedure, predict a substantially less distorted geometry than that predicted by the 6-311G(df,p) basis. Structure 2 is shown to be a true transition structure by vibrational frequency analysis at the CCSD(T)/6-31G(d) level of theory.

**(E) TS(3→5) (4).** In contrast to the conflicting results obtained for 2, all the methods in the present study predict the existence of transition structure 4, linking formylmethylene (3) and ketene (5). In all cases, the geometry is quite nonplanar, with the ∠H<sub>1</sub>C<sub>1</sub>C<sub>2</sub>O dihedral angle being about 94°. The ∠CCO bond angle has opened up considerably to about 125°. As a consequence of the wider ∠CCO angle, the C–O bond distance for the ring-opening side of this structure is now about 2.4 Å. The C–O bond that will eventually become the C=O double bond of ketene has been reduced in length to about 1.2 Å in 4 (*cf.* 1.49 Å in 1 or 1.16 Å in 5). Structure 4 was shown to be a true transition structure by vibrational frequency analysis at the CCSD(T)/6-31G(d) level of theory. It is interesting to note that the magnitude of the imaginary frequency predicted at this level of theory for 4 (409i cm<sup>-1</sup>, Table 1) is in very good agreement with that predicted by Lovejoy *et al.* (400 ± 200i cm<sup>-1</sup>) on the basis of an RRKM analysis of experimental rate data.<sup>5b</sup>

**Energies.** The total energies for the stationary points 1–5 are presented in Table 2. Corresponding relative energies are displayed in Table 3.

Because our best-optimized geometries were obtained at the CCSD(T)/6-311G(df,p) level, the potential energy surface at this level is of special interest. It is depicted schematically in Figure 2, as a plot of relative energy against the ∠CCO angle.

(42) For a detailed discussion of the effect of spin contamination in correlated wave functions, see: Chen, W.; Schlegel, H. B. *J. Chem. Phys.* In press.

**Table 2.** Calculated Total Energies for Structures 1–5<sup>a</sup>

level of theory	oxirene (1)	TS(3→1) (2)	formylmethylene (3)	TS(3→5) (4)	ketene (5)
RHF/6-311G(df,p)	-151.632 73	-151.624 22	-151.655 36	-151.655 22	-151.775 20
MP2/6-311G(df,p)	-152.235 80			-152.219 11	-152.367 45
CCSD(T)/6-31G(d)	-152.064 28	-152.064 27	-152.067 21	-152.056 19	-152.190 28
CCSD(T)/6-31G(d,p)	-152.080 64	-152.080 61	-152.083 97	-152.073 33	-152.207 04
CCSD(T)/6-311G(d,p)	-152.189 37		-152.194 07	-152.186 07	-152.321 05
CCSD(T)/6-311G(df,p)	-152.276 72	-152.276 24	-152.278 39	-152.269 01	-152.405 25
B-LYP/6-311G(df,p)	-152.487 77		-152.499 08	-152.485 32	-152.621 15
Becke3-LYP/6-311G(df,p)	-152.520 95		-152.526 16	-152.518 53	-152.655 68
ZPVE <sup>b</sup>	0.027 98	0.027 89	0.029 70	0.027 69	0.031 71
CCSD(T)/cc-pVTZ <sup>c</sup>	-152.275 66	-152.275 01	-152.276 68	-152.267 06	-152.402 86
BD(T)/cc-pVTZ <sup>c</sup>	-152.275 19	-152.274 36	-152.275 64	-152.266 69	-152.402 52
CCSD(T)/cc-pVTZ(f) <sup>c</sup>	-152.287 01	-152.286 32	-152.287 71	-152.277 59	-152.414 67
CCSD(T)/cc-pVTZ(g) <sup>c</sup>	-152.290 44	-152.289 72	-152.291 32	-152.281 65	-152.417 82

<sup>a</sup> Energies in hartrees. <sup>b</sup> ZPVE calculated at CCSD(T)/6-31G(d). <sup>c</sup> At CCSD(T)/6-311G(df,p) optimized geometries.

**Table 3.** Calculated Energies Relative to Oxirene (1)<sup>a</sup>

level of theory	oxirene (1)	TS(3→1) (2)	formylmethylene (3)	TS(3→5) (4)	ketene (5)
RHF/6-311G(df,p)	0.0	22.3	-59.4	-59.0	-374.0
MP2/6-311G(df,p)	0.0			43.8	-345.6
CCSD(T)/6-31G(d)	0.0	0.0	-7.7	21.2	-330.8
CCSD(T)/6-31G(d,p)	0.0	0.1	-8.7	19.2	-331.9
CCSD(T)/6-311G(d,p)	0.0		-12.3	8.7	-345.7
CCSD(T)/6-311G(df,p)	0.0	1.3	-4.4	20.2	-337.5
B-LYP/6-311G(df,p)	0.0		-29.7	6.3	-350.2
Becke3-LYP/6-311G(df,p)	0.0		-13.6	6.4	-353.7
ZPVE <sup>b</sup>	0.0	-0.2	4.5	-0.8	9.8
CCSD(T)/cc-pVTZ <sup>c</sup>	0.0	1.7	-2.7	22.6	-334.0
BD(T)/cc-pVTZ <sup>c</sup>	0.0	2.2	-1.2	22.3	-334.3
CCSD(T)/cc-pVTZ(f) <sup>c</sup>	0.0	1.8	-1.8	24.7	-335.2
CCSD(T)/cc-pVTZ(g) <sup>c</sup>	0.0	1.9	-2.3	23.1	-334.4
best <sup>c,d</sup>	0.0	1.9	-2.0	23.9	-334.8
best + ZPVE <sup>c,e</sup>	0.0	1.7	2.5	23.1	-325.0

<sup>a</sup> Relative energies in kJ mol<sup>-1</sup>. <sup>b</sup> Calculated at the CCSD(T)/6-31G(d) level. <sup>c</sup> At CCSD(T)/6-311G(df,p) optimized geometries. <sup>d</sup> Mean of CCSD(T)/cc-pVTZ(f) and CCSD(T)/cc-pVTZ(g) values. <sup>e</sup> Including zero-point vibrational energy.

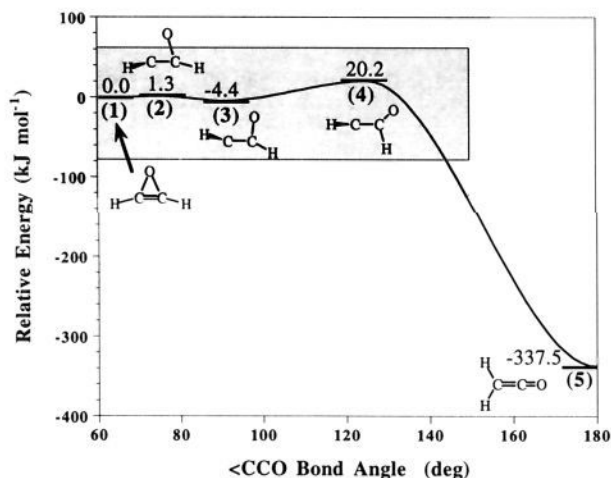


**Figure 2.** Schematic potential energy profile for the rearrangement of oxirene (1) to ketene (5) calculated at the CCSD(T)/6-311G(df,p) level.

It should be stressed that each of the stationary points 1–5 was fully optimized; we have chosen the  $\angle$ CCO bond angle for the  $x$  axis in Figure 2 and subsequent graphs purely for convenience in displaying the results. The boxed area toward the top left corner of Figure 2 is the portion of the surface that is of prime concern in this paper. It covers a region of the surface from a  $\angle$ CCO angle of around 65° (in  $C_{2v}$  oxirene) to an angle of around 150°, and energies, relative to that of the  $C_{2v}$  oxirene structure, of between -80 and +60 kJ mol<sup>-1</sup>.

Figure 2 shows that at the CCSD(T)/6-311G(df,p) level formylmethylene (3) lies in a shallow well, 4.4 kJ mol<sup>-1</sup> lower in energy than oxirene. Conversion of 3 to 1 is predicted to occur

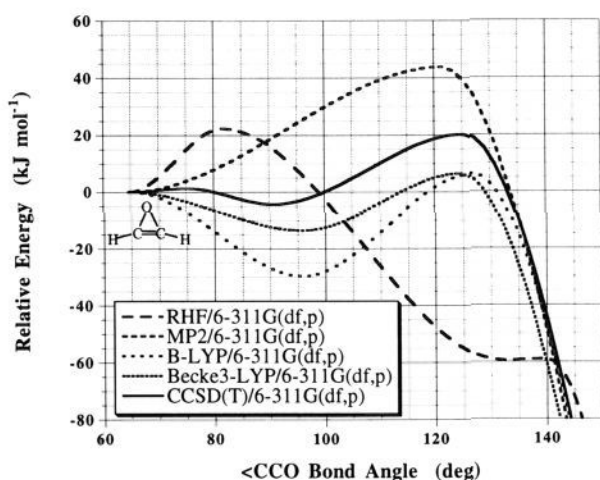


**Figure 3.** Schematic potential energy profiles for the rearrangement of oxirene (1) to ketene (5) calculated at various levels of theory with the 6-311G(df,p) basis. The area shown corresponds to an opening of the  $\angle$ CCO angle from about 65° to 150° as indicated by the boxed area of Figure 2.

with an energy cost of only 5.7 kJ mol<sup>-1</sup>, while the barrier for the formation of ketene from 3 (via 4) is predicted to be 24.6 kJ mol<sup>-1</sup>. Entry into the surface at 3 during a Wolff rearrangement would be expected to lead to facile carbon scrambling, while formation of ketene (5) is achievable without too great an energy impost.

Figure 3 shows the part of the potential energy surface corresponding to the boxed area of Figure 2, again with the 6-311G(df,p) basis, but this time with a selection of levels of theory. Immediately apparent is the poor performance of RHF

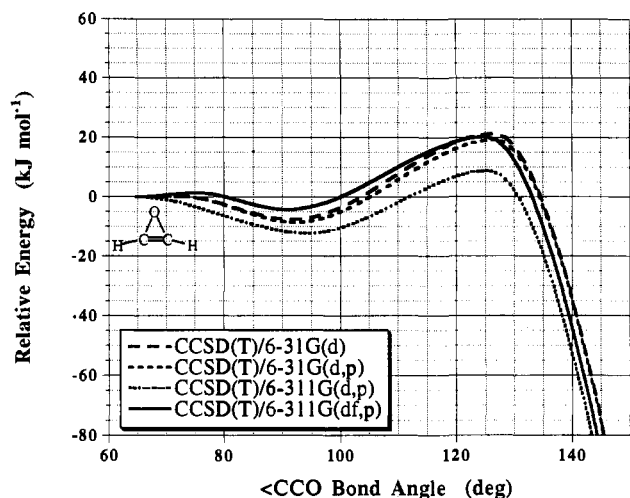


**Figure 4.** Schematic potential energy profiles for the rearrangement of oxirene (**1**) to ketene (**5**) calculated with the CCSD(T) method and a variety of basis sets. The area shown corresponds to an opening of the  $\angle$ CCO angle from about  $65^\circ$  to  $150^\circ$  as indicated by the boxed area of Figure 2.

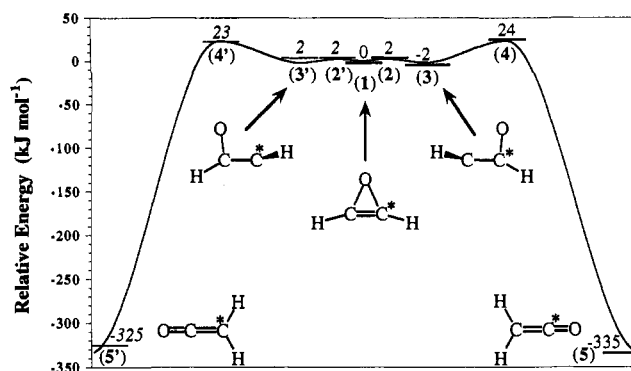
theory, which produces a surface quite different from that obtained with any of the other methods. The MP2 and DFT results have qualitative deficiencies that are less significant, the former predicting that formylmethylene (**3**) is unstable while both of the DFT procedures predict that oxirene (**1**) is not a stable structure. In addition, the DFT procedures predict energies for formylmethylene (**3**) relative to oxirene (**1**) that appear much too low.

Figure 4 displays the same region of the surface with the CCSD(T) procedure and several different basis sets. The main observation is that the surfaces are all quite similar. The largest differences compared with CCSD(T)/6-311G(df,p) are found with the 6-311G(d,p) basis: at the CCSD(T)/6-311G(d,p) level of theory, the  $C_2$  oxirene structure has one imaginary frequency.

Table 3 shows the results of single-point energy calculations on the CCSD(T)/6-311G(df,p) optimized structures with larger basis sets and with an alternative high level correlation procedure (BD(T)). Only minor changes in the calculated relative energies are observed with these increasingly sophisticated procedures. Neither the change from CCSD(T) to BD(T) nor the incorporation of an additional f or an initial g function in the cc-pVTZ basis set are found to have a significant effect on the calculated relative energies. Thus, the higher level calculations all predict that formylmethylene (**3**) lies in a shallow well, lying 1–3 kJ mol<sup>-1</sup> lower in energy than oxirene (**1**), and that the barrier for isomerization of **3** to **1** is 3–5 kJ mol<sup>-1</sup>. An energy barrier of 23–27 kJ mol<sup>-1</sup> is found for the conversion of **3** to **5**.

We take as our best estimates of the (vibrationless) relative energies of structures **1**–**5** the mean of the CCSD(T)/cc-pVTZ(f) and CCSD(T)/cc-pVTZ(g) values, as displayed in Table 3 and Figure 5. These show oxirene (**1**) and formylmethylene (**3**) to lie in individual potential wells, separated by a small barrier at **2**.

Also included in Table 3 and Figure 5 are relative energies at our best level but in which zero-point vibrational energy (ZPVE) corrections, calculated at the CCSD(T)/6-31G(d) level of theory, have been incorporated. With zero-point energies included, it can be seen that the energy of **3** lies marginally above that of **2**, i.e. **3** is predicted to collapse without a barrier to **1**. This reversal of the energy ordering that accompanies the incorporation of zero-point vibrational energies underlies the fact that the potential



**Figure 5.** Schematic potential energy profile, corresponding to our best calculated values (see text), depicting carbon scrambling during a Wolff rearrangement. Energies of stationary points, shown as bold lines (without ZPVE corrections) or as thin lines (with ZPVE corrections, as calculated at the CCSD(T)/6-31G(d) level) are given in normal or *italics* text, respectively.

surface in the region of **1**, **2**, and **3** is extremely flat. Uncertainties in the equilibrium surface and in the calculated zero-point energies mean that we cannot state categorically whether the experimentally observed species will correspond to **1** or **3**. The zero-point energy treatment in particular is only very approximate because of the use of frequencies calculated at a lower, albeit substantial, theoretical level (CCSD(T)/6-31G(d) instead of CCSD(T)/cc-pVTZ(f) or CCSD(T)/cc-pVTZ(g)) and neglect of anharmonicity effects (for a motion that is clearly quite highly anharmonic). Our main conclusion is that the potential surface is very flat and there should be a large-amplitude, low-energy motion linking structures in the vicinity of **1**, **2**, and **3**.

Figure 5 clearly demonstrates that entry into the Wolff rearrangement at the formylmethylene stage (**3**) will readily present opportunities for carbon scrambling to take place with very little or no energy cost. The subsequent formation of ketene (**5**) takes place over an energy barrier of 21 kJ mol<sup>-1</sup>. Our predicted energy for transition structure **4** relative to ketene (**5**) is 348 kJ mol<sup>-1</sup>, in excellent agreement with the isomerization threshold for ketene (340 kJ mol<sup>-1</sup>) calculated using an RRKM analysis of experimental rate data by Lovejoy *et al.*<sup>5b</sup>

## Summary and Conclusions

We have calculated the structures and energies for various species thought to be involved in the Wolff rearrangement. Our best geometries were determined at the CCSD(T)/6-311G(df,p) level of theory, and at this level the potential surface in the region of oxirene and formylmethylene is extremely flat. Higher-level single-point energy calculations using the cc-pVTZ, cc-pVTZ(f), and cc-pVTZ(g) basis sets with the CCSD(T) procedure and the cc-pVTZ basis with the BD(T) method result in only minor changes to the relative energies. Our results clearly support the participation of oxirene in the Wolff rearrangement. Entry to the rearrangement at the formylmethylene stage results in an opportunity for carbon scrambling through the symmetric oxirene structure with very little energy cost. This is in accord with experimental observations. Our calculated threshold energy for scrambling of carbon atoms in ketene (348 kJ mol<sup>-1</sup>) is in excellent agreement with the experimental estimate (340 kJ mol<sup>-1</sup>).

**Acknowledgment.** A.P.S., R.H.N., and L.R. thank the Australian National University Supercomputer Facility for a generous allocation of computer time on the Fujitsu VP2200. H.F.S. thanks the U.S. Department of Energy for support.